

# Vibrational excitation of acetylene by positron impact

## The totally symmetric modes at near-threshold energies

J. Franz<sup>1,a</sup> and F.A. Gianturco<sup>1,b</sup>

Department of Chemistry, University of Rome La Sapienza, Piazzale A. Moro 5, 00185 Rome, Italy

Received 30 March 2006 / Received in final form 20 April 2006

Published online 18 May 2006 – © EDP Sciences, Società Italiana di Fisica, Springer-Verlag 2006

**Abstract.** Vibrationally inelastic quantum calculations are carried out at low collision energies for the scattering of a beam of positrons off acetylene gaseous molecules. The normal mode analysis is assumed to be valid and the relative fluxes into the C–C and C–H symmetric vibrational modes are computed within a Body-Fixed (BF) formulation of the dynamics by solving the relevant vibrational Coupled Channels (VCC) equations. The clear dominance of the C–C mode is observed near threshold and the implications of this finding are briefly considered in relation to more global indicators like the average vibrational energy transfer indices as obtained in the present work.

**PACS.** 34.10.+x General theories and models of atomic and molecular collisions and interactions (including statistical theories, transition state, stochastic and trajectory models, etc.) – 36.10.Dr Positronium, muonium, muonic atoms and molecules – 82.30.Gg Positronium chemistry

## 1 Introduction

There has been a marked increase, in the last few years, of an appreciation for the scientific potentials and fundamental interests of low-energy antimatter physics and chemistry, both for its technological applications and for its basic significance. Reasons for its fundamental importance revolve around the formation of neutral antihydrogen atoms (a test of QED validity), the existence of possible bound states to simple or to complex molecules (the positronic analogue of anionic chemistry) and the variety of mesoscopic effects related to the formation of positronium (Ps) compounds, of Ps<sub>2</sub> molecules, of Bose-condensed gases of Ps atoms or the formation of electron-positron plasmas [1–4]. The positrons further offer complementary ways of producing molecular ions, of testing atomic clusters or nanoparticles in general and invariably require a better knowledge of their interactions with atoms and molecules [5,6].

The further comparison of dynamical attributes obtained in molecular gases using both electrons and positrons as probes [7] helps us to shed more light on the interplay of the various interaction forces which preside over the low-energy scattering cross-sections (elastic and inelastic) and provides a more quantitative basis for the

relative merits and surprises yielded by antimatter phenomena.

In the present study we shall focus on a specific area of experimental interest, i.e. the excitation of vibrational internal molecular states by positron impact, in order to see if accurate calculations like those we shall describe below are able to predict which specific molecular modes will be more efficiently “heated” by the impinging positron projectiles.

The work will be divided as follows: the next section briefly reviews our treatment of vibrationally inelastic collisions and our modelling of the positron-molecule interaction potentials. Section 3 will present our findings and compare the behaviour of both the C–C and C–H stretching excitations at energies near their thresholds. Section 4 will provide our conclusions and future plans.

## 2 The computational approach

In the analysis and computational formulation of the scattering process within a multichannel approach we will, however, restrict our study to the vibrational channels after summing over final rotational states and averaging over the initial ones. In other words, we will be interested in those processes which occur below the “reactive” channels of either positron annihilation or of positronium (Ps) formation. In the acetylene molecular gas the first ionization potential is at 11.41 eV and therefore the Ps formation threshold is located at 4.6 eV. We shall therefore focus

<sup>a</sup> *Present address:* Department of Physics and Astronomy, University College London, Gower Street, London, WC1E6BT, UK.

<sup>b</sup> e-mail: fa.gianturco@caspur.it

on the low-energy behaviour of the vibrational excitation processes below that formation threshold.

The details of the present approach have been already reported in our previous work [8,9], so we shall here provide the reader with only a brief reminder of them. In order to obtain vibrational excitation cross-sections for positron scattering from polyatomic molecules we need to solve the Schrödinger equation of the total system to yield the total wavefunction  $\Psi$  at a fixed value of the total energy  $E$ . It should also be noted that no Ps formation channel is considered throughout the present calculations as this process is estimated to be absent at the energies we are considering.

We can also assume that the orientation of the target molecule is being kept fixed during the collision since molecular rotations are slower when compared with the velocity of the projectile at the energies we are considering. This is usually called the fixed-nuclear orientation (FNO) approximation [10], and corresponds to ignoring the rotational Hamiltonian of the total system. The actual rotational levels are therefore included by averaging over the initial levels and summing over the final ones within the Body-Fixed (BF) formulation of that problem [10]. Then, the total wavefunction could be generally expanded as follows

$$\Psi(\mathbf{r}_p | \mathbf{R}) = r_p^{-1} \sum_{l\nu n} u_{l\nu n}(r_p) X_{l\nu}(\hat{\mathbf{r}}_p) \chi_n(\mathbf{R}). \quad (1)$$

Here,  $\chi_n$  is the vibrational wavefunction of the molecule with the vibrational quantum number  $n \equiv (n_1, \dots, n_N)$  with  $N$  representing the total number of normal vibrational modes of the target molecule. The variables  $\mathbf{R}$  and  $\mathbf{r}_p$  now denote the molecular nuclear geometry and the position vector of the positron from the center-of-mass (c.o.m.) of the target, respectively. The unknown functions  $u_{l\nu n}$  describe the radial coefficients of the wavefunction of the incident particle and the  $X_{l\nu}$  are the symmetry-adapted angular basis functions [11]. In this paper,  $\nu$  in equation (1) stands for the indices ( $p\mu h$ ) collectively, and  $p$  stands for the chosen irreducible representation,  $\mu$  distinguishes the component of the basis if its dimension is greater than one, and  $h$  does that within the same set of ( $p\mu$ ).

After substituting equation (1) into the equation of the total collision system under the FNO approximation, we obtain for  $u_{l\nu n}(r_p)$  a set of full close-coupling equations which now also include vibrational channels. These are called the body-fixed vibrational close-coupling (BF-VCC) equations [8,9],

$$\left\{ \frac{d^2}{dr_p^2} - \frac{l(l+1)}{r_p^2} + k_n^2 \right\} u_{l\nu n}(r_p) = 2 \sum_{l'\nu'n'} \langle l\nu n | V | l'\nu'n' \rangle u_{l'\nu'n'}(r_p), \quad (2)$$

where  $k_n^2 = 2(E - E_n^{vib.})$  with  $E_n^{vib.}$  being the energy of the specific molecular vibration we are considering. Any of the elements of the interaction matrix in equation (2)

is given by

$$\langle l\nu n | V | l'\nu'n' \rangle = \sum_{l_0\nu_0} \int d\mathbf{R} \{ \chi_n(\mathbf{R}) \}^* V_{l_0\nu_0}(r_p | \mathbf{R}) \{ \chi_{n'}(\mathbf{R}) \} \\ \times \int d\hat{\mathbf{r}}_p X_{l\nu}(\hat{\mathbf{r}}_p)^* X_{l_0\nu_0}(\hat{\mathbf{r}}_p) X_{l'\nu'}(\hat{\mathbf{r}}_p). \quad (3)$$

In the present study the employed bound state wavefunctions were obtained within the harmonic approximation and the coupling potential was generated over the required range of normal coordinates.

This method is essentially a generalization of the method proposed long ago (called the ‘‘hybrid theory’’) for the simple case of a diatomic molecule [12]. When solving equation (2) under the boundary conditions that the asymptotic form of  $u_{l'\nu'n'}$  is represented by a sum containing the incident plane wave of the projectile and the outgoing spherical wave, we obtain the  $K$ -matrix elements. Therefore, the integral cross-section for the vibrationally inelastic scattering is given by

$$Q(n \rightarrow n') = \frac{\pi}{k_n^2} \sum_{l\nu} \sum_{l'\nu'} |T_{l'\nu'n'}^{l\nu n}|^2 \quad (4)$$

where  $T_{l'\nu'n'}^{l\nu n}$  is the  $T$ -matrix element.

The interaction potential ( $V$ ) between the impinging positron and the molecular target is represented here by us in the form of a local potential. Thus,  $V$  is described by the sum of the repulsive electrostatic ( $V_{st}$ ) and the attractive positron correlation-polarization ( $V_{pcp}$ ) terms. To describe the latter contribution we have employed over the years [8, 9] the simple parameter-free model potential introduced by Boronski and Nieminen [13] for the short-range region of  $r_p$ , and have connected it smoothly with the asymptotic form of the polarization potential  $-\alpha_0/2r_p^4$  with  $\alpha_0$  being the spherical dipole polarizability of the target.

In addition, one can also adopt a simpler computational method which has often been employed to treat vibrational excitation. It is called the adiabatic nuclear vibration (ANV) approximation (see, e.g., [14]) where no direct positron-nuclei dynamical coupling like in equation (3) is active during the scattering process. The  $T$ -matrix elements are thus obtained as simple expectation values from a quadrature with respect to the fixed-nuclei (FN)  $T$ -matrix for each specific normal mode wavefunction of the target,

$$T_{l'\nu'n'}^{l\nu n} = \int d\mathbf{R} \{ \chi_{n'}(\mathbf{R}) \}^* T_{l'\nu'}^{l\nu}(\mathbf{R}) \{ \chi_n(\mathbf{R}) \}. \quad (5)$$

In earlier calculations on the CH stretching vibrational excitation of acetylene by positron impact [15] we had employed the ANV approximation: it is therefore of interest to see how well it behaves when one moves closer to the threshold opening of that inelastic channel.

### 3 Results and discussion

To actually measure state-resolved, vibrationally inelastic cross-sections has posed considerable difficulties for

conventional, moderator-based positron beams, especially because of the inherent methodological limitations of the energy resolution since, for vibrational energy transfer measurements, the corresponding levels could lie anywhere between a few meV and up to 500 meV.

Hence, there have been only a few attempts at measuring vibrational excitation cross-sections with conventional beams, using time-of-flight detection [16,17].

Later, subsequent work was carried out using trap based beams and it has managed to fully resolve the  $\nu_3$  mode of  $\text{CF}_4$  [18] and to further obtain vibrational excitation cross-sections for  $\text{CO}$ ,  $\text{H}_2$ ,  $\text{CO}_2$ ,  $\text{CH}_4$  and  $\text{CF}_4$  [19,20].

In spite of the variety of systems which have been examined in recent years, however, no experimental data are available for the vibrational excitation of  $\text{C}_2\text{H}_2$ , although several studies concerning positron interactions for that molecular gas have already attempted. For example, the vibrational enhancement of the annihilation rates has been detected experimentally by Gilbert et al. [21] while measurement of total cross-sections without resolving vibrational excitation were reported by reference [22].

On the theoretical side, the elastic cross-section behaviour has been studied before [23–25] and we have further investigated the appearance of low-energy virtual states when the  $\text{C}_2\text{H}_2$  molecule is vibrationally excited [26]. We have also modelled the  $Z_{eff}$  enhancement in the presence of vibrationally excited target molecules [27] and, more recently, we have analysed the threshold features of the CH stretching mode by calculating the relevant cross-sections within the ANV approximation [15].

In the present study the molecular geometry has been optimized at the Single-Determinant, Hartree-Fock level as implemented in the program package GAUSSIAN 98 [28] using the D95\*\* basis set. The final energy value turned out to be  $-76.8325443$  Hartree. The  $r_{CC}$  distance was found to be  $1.191 \text{ \AA}$  and the  $r_{CH}$  was  $1.060 \text{ \AA}$ , to be compared with the experimental values [30] of  $1.203 \text{ \AA}$  and  $1.060 \text{ \AA}$ , respectively. The two symmetric stretching modes, the C–H stretch and the  $\text{C}\equiv\text{C}$  stretch, were computed as outlined in our earlier work [29] and the corresponding pseudo 1D potential energy curves extended over four vibrational bound levels. The spacing between the C–H stretch levels was of  $3681.0 \text{ cm}^{-1}$ , while the one for the  $\text{C}\equiv\text{C}$  stretch was of  $2205.0 \text{ cm}^{-1}$ . They are to be compared with the experimental values [30] of  $3372.5 \text{ cm}^{-1}$  for the  $\nu_{CH}$  and of  $1973.3 \text{ cm}^{-1}$  for  $\nu_{CC}$ .

The scattering calculations followed the coupled-channel approach discussed in the previous section and the interaction potential was matched at long range with the dipole polarizability coefficient that was calculated over the same range of molecular geometries as the normal modes of above. Care was taken to rescale its values to match the experimental value at the equilibrium geometry (28.68 D), which was the only available experimental datum (calculated value: 15.89 D).

The range of computed  $r_{CC}$  and  $r_{CH}$  values went according to the data given by Table 1.

The multipolar expansion of the potential was carried out up  $\lambda_{max} = 48$ , while the scattering wavefunction re-

**Table 1.** Range of geometries used in the calculation of the vibrational nominal modes.

variable	lower limit	upper limit
CC-stretch		
$r_{CC}$	$1.011 \text{ \AA}$	$1.372 \text{ \AA}$
$r_{CH}$	$0.993 \text{ \AA}$	$1.127 \text{ \AA}$
CH-stretch		
$r_{CC}$	$1.121 \text{ \AA}$	$1.262 \text{ \AA}$
$r_{CH}$	$1.336 \text{ \AA}$	$0.784 \text{ \AA}$

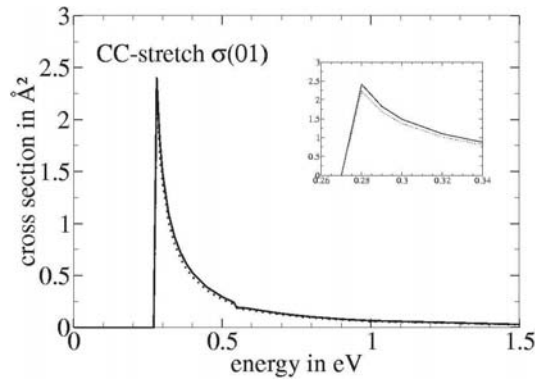
tained partialwave values up to  $l_{max} = 24$ . The radial integration grid was extended up to 978 points in all calculations.

The three panels of Figure 1 report the partial, integral cross-sections for the excitations among the lowest three levels of the  $\text{C}\equiv\text{C}$  stretching mode. One clearly sees there that, by the time we include the highest potential multipoles the cross-sections have converged rather well: the addition of further vibrational coupled channels beyond  $n = 2$  did not change their values.

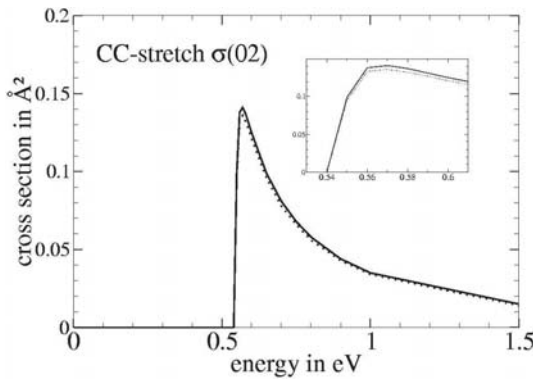
As expected, the  $\sigma_{0\rightarrow 1}$  excitation yields the largest partial cross-section while all of the excitation cross-sections show the same energy dependence: the appearance of a strong threshold peak and the rapid decrease of the excitation probabilities within 2–3 eV above thresholds.

The corresponding superelastic collisions are shown by Figure 2, where one sees how much larger they turn out to be near threshold, an indication of the amplifying effect due to virtual state formation as surmised by our previous work on this molecule [26,27]. One also detects from the energy behaviour that such enhancement effect, as expected, essentially disappears at collision energies away from threshold.

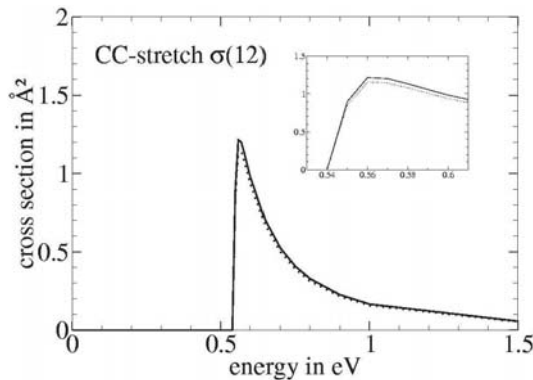
The corresponding partial excitation cross-sections for the symmetric C–H stretching mode are reported by Figure 3, where the three panels show, from top to bottom, the  $\sigma_{0\rightarrow 1}$ , the  $\sigma_{0\rightarrow 2}$  and the  $\sigma_{1\rightarrow 2}$  excitation processes. The single-quantum excitations (top and bottom panels) are occurring more efficiently than the  $\Delta\nu = 2$  process, a feature that was also present in the results of Figure 1 for the  $\text{C}\equiv\text{C}$  mode. In the case of the C–H stretch, as in the previous data of Figure 1, we see that the threshold peak associated with the  $(0 \rightarrow 1)$  transition decays very rapidly and the same occurs for the other two excitation processes presented in Figure 3. In other words, all excitation mechanisms act very close to the threshold energies and become very rapidly less efficient as the energy of the impinging positron increases. Given the weak coupling which exists between the projectile and the nuclear motion, we therefore see confirmed what had been observed thus far in all other inelastic cross-section behaviour [25, 29], i.e. that the energy transfer efficiency is largest when the positron low residual energy allows for much longer interaction times. On the other hand,  $e^+$  projectiles which impact at energies much larger than the threshold energy for that channel cause a much reduced energy transfer effect [26].



(a)



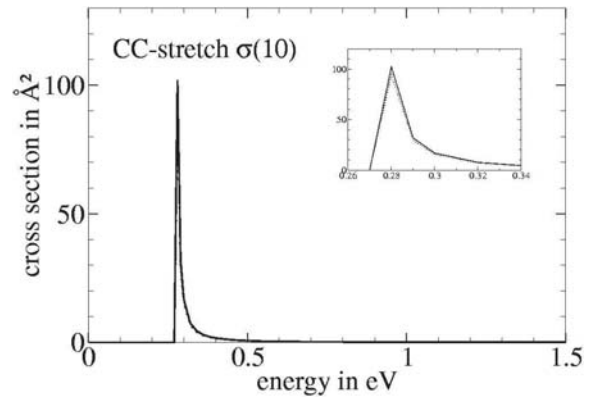
(b)



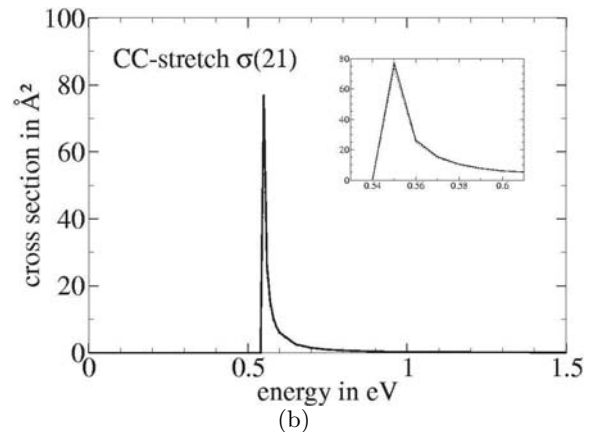
(c)

**Fig. 1.**  $\Delta n = 1$  vibrational excitation cross-sections for the CC-stretch vibration. The levels involved are  $n = 0, 1$  and  $2$ . The results for different partial wave expansions are shown. The solid line refers to  $l = 12$ . The dotted ( $l = 18$ ) and dashed ( $l = 24$ ) lines nearly coincide so only  $l = 18$  is shown in the figures.

The data given by Figure 4 present the partial cross-sections for the superelastic (vibrational cooling) collisions from the first two vibrationally excited levels: as seen before, the size of such partial cross-section changes dramatically when one moves from the  $v = 1$  to the  $v = 2$  initial states. Furthermore, we see that here again the efficiency of the vibrational cooling of the target molecule dies out very rapidly as the collision energy increases: the same type of mechanism, therefore, is present here as it



(a)



(b)

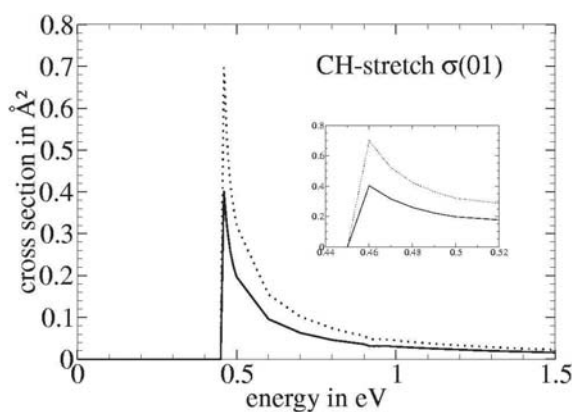
**Fig. 2.** Vibrational de-excitation cross-sections for the CC-stretch vibration. The results for different partial wave expansions are shown. The dotted ( $l = 18$ ) and dashed ( $l = 24$ ) line nearly coincide.

was discussed before. On the whole, however, the cooling cross-sections are by 1 or 2 orders of magnitude larger than the excitation cross-sections.

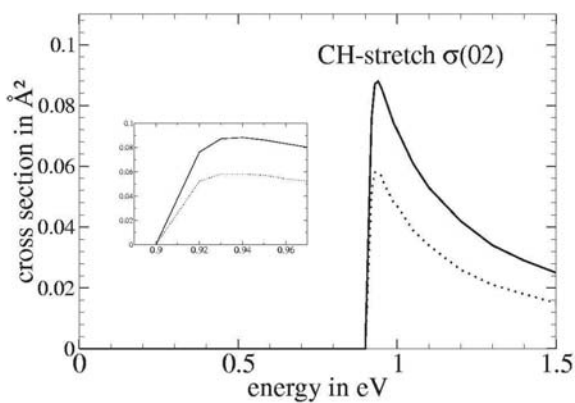
It is also of interest to compare the excitation behaviour for the two modes we have discussed in the present work and to possibly indicate which of the two may provide the more efficient path to molecular “heating” by low-energy positrons.

The previous results for the excitation cross-sections are therefore compared in the three panels of Figure 5. We have reported there calculations carried out for the  $(0 \rightarrow 1)$  (top panel),  $(0 \rightarrow 2)$  (middle) and  $(1 \rightarrow 2)$  (bottom panel). The  $C\equiv C$  stretching excitation process is clearly seen to yield the larger excitation cross-sections between the two symmetric stretching modes we have analysed in Figure 5. The lower excitation, in fact, is at threshold about a factor of five larger for the  $C\equiv C$  bond than it is for the  $C-H$  bond and this ratio is qualitatively reduced to three for the two excitation cross-sections reported by the other panels of the same figure.

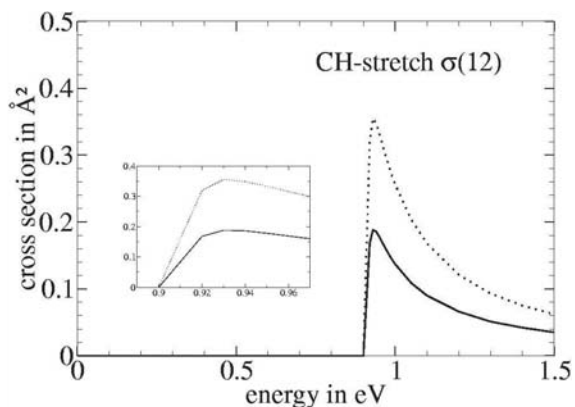
In other words, we see that to excite a mode with less energy needed in the transition is favored in cases where no permanent dipole moment in the target molecule plays a dominant role in the scattering and where the modes



(a)



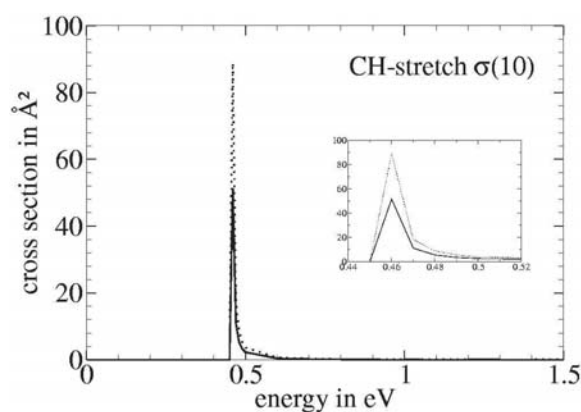
(b)



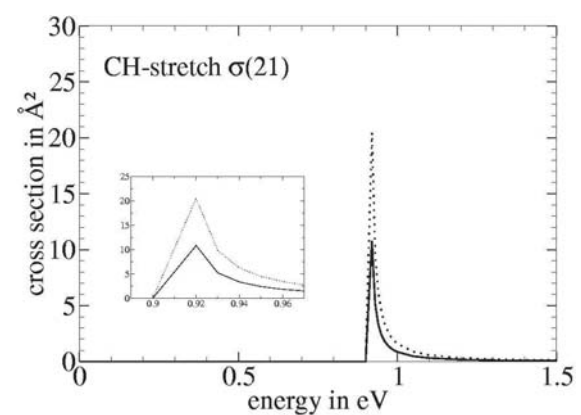
(c)

**Fig. 3.** Same as in Figure 1 but for the CH-stretch vibrations. The results for different partial wave expansions are shown. The solid line refers to  $l = 12$ . The dotted ( $l = 18$ ) and dashed ( $l = 24$ ) lines nearly coincide so only the  $l = 18$  calculation is shown in the figures.

considered are IR inactive as in our case. Further, we can say that the weak distortion induced into the molecular nuclear motion by the positron impact favors excitation where a smaller amount of energy is transferred, as is the case for the  $C\equiv C$  bond. Thus, the  $C\equiv C$  distortion process is seen to occur more efficiently in spite of the multiple-bonding nature of that configuration, while the



(a)



(b)

**Fig. 4.** Same as in Figure 2 but for the CH-stretch vibrations. The results for different partial wave expansions are shown. The solid line refers to the  $l = 12$  calculations. The dotted ( $l = 18$ ) and dashed ( $l = 24$ ) lines nearly coincide so only the  $l = 18$  is shown.

stronger C–H bond is less efficiently affected by the impacting positron.

On the other hand, at collision energies where both channels are opened the two excitation cross-sections show at first ( $0.45 < E_{coll} < 0.6$  eV) a dominance of the (C–H) excitation and then, as the  $E_{coll}$  increases, the two excitation cross-sections become comparable in size. This finding is also confirmed by the data in the middle and lower panels of Figure 5.

The data reported by Figure 6 further show the energy dependence, for both the symmetric modes, of the average energy transfer index from the  $\nu = 0$  initial levels of the C–H and  $C\equiv C$  stretching excitation. Such an index is defined as [29]:

$$\langle \Delta E \rangle_{vib}^{n=0} = \frac{\sum_{i \neq 0}^{all} \Delta E_{0 \rightarrow i} \times \sigma_{0 \rightarrow i}}{\sum_{i \neq 0}^{all} \sigma_{0 \rightarrow i}} \quad (6)$$

and provides an indicator of the efficiency with which the positron beam is transversing the neutral gas and is thus providing vibrational heating of the molecules in it by collisional energy transfer.

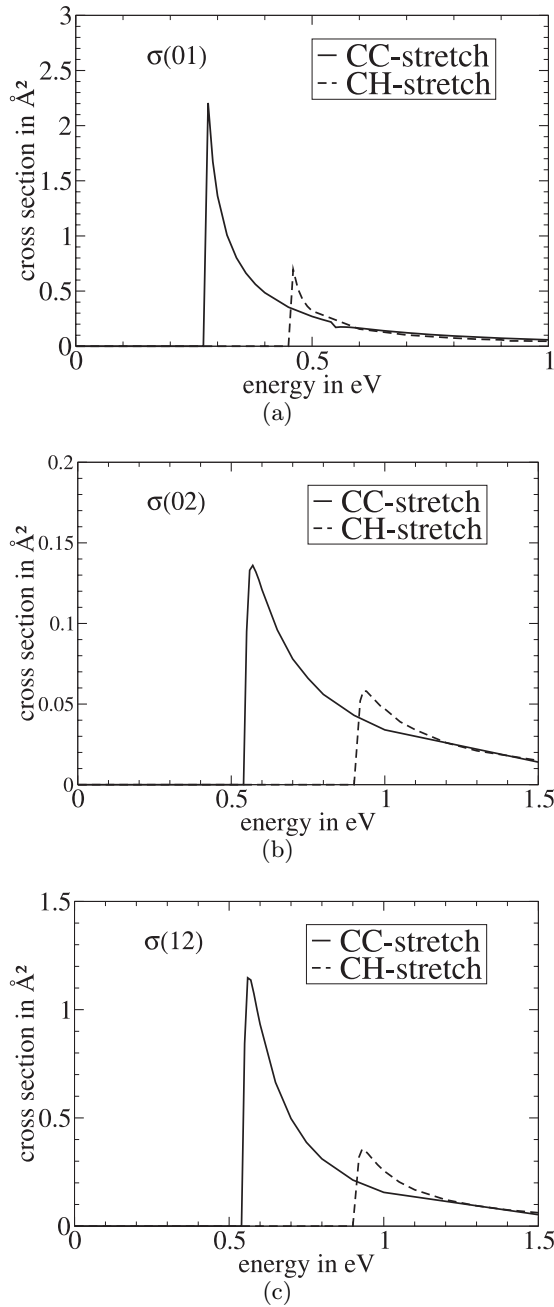


**Fig. 5.** Comparison of vibrational excitation cross-sections for the CH-stretch (solid line) and the CC-stretch (dashed line). Only results for  $l = 24$  are shown.

The energy spacing values,  $\Delta E_{0 \rightarrow i}$ , were obtained within the harmonic approximation, using the frequency values already mentioned in the previous section.

It is interesting to see the comparative effects on the index behaviour of two conflicting features of the collision process: the amount of energy being transferred in a single scattering event (larger for the CH stretching mode) and the size of the quantum dynamical channel which causes the transfer (i.e. the partial inelastic cross-sections, larger for the  $\text{C}\equiv\text{C}$  excitation). At the very low collision ener-

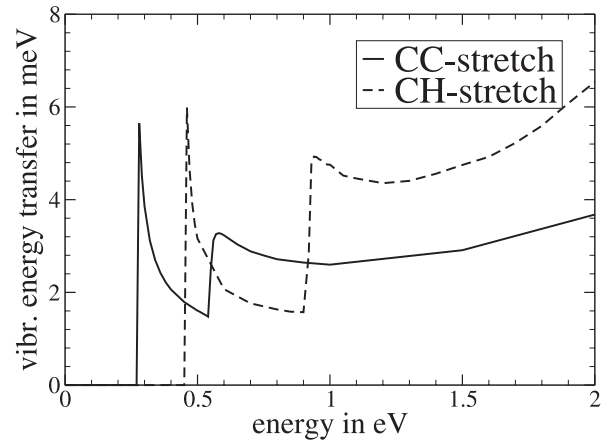


**Fig. 6.** Computed average vibrational energy transfer index defined by equation (6). The results refer to CC excitation (solid line) and to CH excitation (dashes).

gies right after the threshold openings we see that the CC mode excitation dominates the energy transfer efficiency. On the other hand, as the collision energy increases we see that the CH mode is increasingly providing larger efficiency indices and clearly dominates the energy transfer process.

#### 4 Present conclusions

We have carried out quantum scattering calculations for the vibrationally inelastic cross-sections of the two stretching modes of the  $\text{C}_2\text{H}_2$  molecular gas by impact of low-energy positrons. The calculations were performed at the coupled-channel level (BF-VCC) and therefore allowed us to obtain realistic cross-sections down to the threshold openings for both excitation processes (i.e. from about 28 meV and about 450 meV, respectively).

Our results at thresholds clearly indicate the dominance of the  $\text{C}\equiv\text{C}$  excitation cross-section size over that for the  $\text{C}-\text{H}$  bond excitation mechanism, a feature which thus provides average energy transfer indicators close to thresholds which are larger for the  $\text{C}\equiv\text{C}$  symmetric stretching mode than for the  $\text{C}-\text{H}$  mode. One also sees from the present results that all excitation processes exhibit a very marked threshold peak for both modes and for all the different transitions between the lower levels. Those findings suggest that positron excitation of vibrational modes is a fairly inefficient process which chiefly occurs close to threshold energies and which becomes almost negligible when the interaction times are shorter at the higher positron collision energies away from thresholds.

It is also interesting to note that, although the CH stretching mode shows in this system the presence of fairly small cross-sections of about  $0.7 \text{\AA}^2$  at the threshold peak, similar symmetric stretches in the  $\text{CH}_4$  molecule [8] showed threshold peaks around  $0.08 \text{\AA}^2$  and the  $\text{H}_2$  molecules exhibited an excitation peak of about  $0.1 \text{\AA}^2$  [31]. Even the CO molecule was observed to have

an excitation peak of about  $0.25 \text{ \AA}^2$  [32], all values which are smaller than the present findings for the threshold behaviour of the CH spectra in acetylene. Thus, one can say that, given the basic difficulty for the light positron to excite molecular vibrational modes, the present calculations indeed indicate that the  $\text{C}_2\text{H}_2$  gas should be among the most likely to undergo vibrational heating by positron collisional energy transfer mechanisms to its  $\text{C}\equiv\text{C}$  and  $\text{C-H}$  vibrational modes.

Another interesting result is given by the evaluation of the average vibrational energy transfer indicators: in the region of scattering energies where both channels are open, the data in Figure 6 indicate an initial dominance of the (CH) excitation mode, followed by larger (CC) efficiency at intermediate energized ( $0.6 < E_{\text{coll}} < 0.9 \text{ eV}$ ) with a clear dominance of the heating efficiency of the (CH) mode at energies above 1 eV.

The financial support of the CASPUR Supercomputing Center, of the Research Committee of the University of Rome "La Sapienza" and of the EU Network "EPIC" (Electron and Positron Induced Chemistry) no. HPRN-CT-202-00286 are gratefully acknowledged. One of us (J.F.) also thanks the EPIC Network for the award of a Young Researcher Fellowship at the University of Rome "La Sapienza" during the year 2005.

## References

1. M. Charlton, J.M. Humbertson, *Positron Physics* (Cambridge, Cambridge University Press, 2001)
2. *Positron Annihilation Studies in Fluids*, edited by S.C. Sharma (World Scientific, Singapore, 1988)
3. *New Directions in Antimatter Chemistry and Physics*, edited by C.M. Surko, F.A. Gianturco (Kluwer, Dordrecht, Holland, 2001)
4. T.C. Griffith, G.R. Heyland, *Phys. Rep.* **39**, 169 (1978)
5. W.E. Kauppila, T.S. Stein, *Adv. At. Mol. Opt. Phys.* **26**, 1 (1990)
6. C. M. Surko, G.F. Gribakin, S.J. Buckman, *J. Phys. B: At. Mol. Opt. Phys.* **38**, R57 (2005)
7. M. Kimura, O. Sueoka, A. Hamada, Y. Itikawa, *Adv. Chem. Phys.* **111**, 537 (2000)
8. T. Nishimura, F.A. Gianturco, *Nucl. Inst. Meth. B* **192**, 17 (2002)
9. T. Nishimura, F.A. Gianturco, *Phys. Rev. A* **65**, 062703 (2002)
10. E.g. see: Y. Itikawa, *Int. Rev. Phys. Chem.* **16** 155 (1997)
11. P.G. Burke, N. Chandra, F.A. Gianturco, *J. Phys. B* **5**, 2212 (1972)
12. N. Chandra, A. Temkin, *Phys. Rev. A* **13**, 188 (1976)
13. E. Boronski, R.M. Nieminen, *Phys. Rev. B* **34**, 3820 (1986)
14. M. Cascella, R. Curik, F.A. Gianturco, *J. Phys. B* **34**, 705 (2001)
15. T. Nishimura, F.A. Gianturco, *Nucl. Inst. Meth. B.* **221**, 24 (2004)
16. M. Kimura, M. Tachikawa, H. Takaki, O. Sueoka, *Phys. Rev. Lett.* **80**, 3936 (1998)
17. M.I. Kawada, O. Sueoka, M. Kimura, *J. Chem. Phys.* **112**, 7057 (2000)
18. S.J. Gilbert, R.G. Greaves, C.M. Surko, *Phys. Rev. Lett.* **82**, 5032 (1999)
19. J.P. Sullivan, S.J. Gilbert, C.M. Surko, *Phys. Rev. Lett.* **86**, 1494 (2001)
20. J.P. Sullivan, S.J. Gilbert, J.P. Marler, L.D. Barnes, S.J. Buckman, C.M. Surko, *Nucl. Inst. Meth. B* **192**,3 (2002)
21. S.J. Gilbert, L.D. Barnes, J.P. Sullivan, C.M. Surko, *Phys. Rev. Lett.* **88**, 043201 (2002)
22. O. Sueoka, S. Mori, *J. Phys. B* **22**, 963 (1989)
23. C.R.C. de Carvalho, M.T. do N. Varella, M.A.P. Lima, E.P. da Silva, J.S.E. Germano, *Nucl. Inst. Meth. B* **171**, 33 (2000)
24. C.R.C. de Carvalho, M.T. do N. Varella, M.A.P. Lima, E.P. da Silva, *Phys. Rev. A* **68**, 062706 (2003)
25. A. Occhigrossi, F.A. Gianturco, *J. Phys. B* **36**, 1383(2003)
26. T. Nishimura, F.A. Gianturco, *Europhys. Lett.* **68**, 377 (2004)
27. F.A. Gianturco, T. Nishimura, *Phys. Rev. A* **72**, 022706(2005)
28. M.J. Frisch et al. Gaussian 98, Revision A.7, Gaussian Inc., Pittsburg PA, 1998
29. T. Nishimura, F.A. Gianturco, *J. Phys. B* **35**, 2873 (2002)
30. G. Herzberg, *Molecular Spectra and Molecular Structures. III: Electronic Spectra and Electronic Structure of Polyatomic Molecules* (D. van Nostrand, Princeton, N.J., 1966)
31. F.A. Gianturco, T. Mukherjee, *Phys. Rev. A* **64**, 024703 (2001)
32. F.A. Gianturco, T. Mukherjee, P. Paoletti, *Phys. Rev. A* **56**, 3638 (1997)